

Use of Molten Alkali-Metal Polythiophosphate Fluxes for Synthesis at Intermediate Temperatures. Isolation and Structural Characterization of ABiP₂S₇ (A = K, Rb)

Timothy J. McCarthy and Mercuri G. Kanatzidis*[†]

Department of Chemistry and the
Center for Fundamental Materials Research
Michigan State University
East Lansing, Michigan 48824

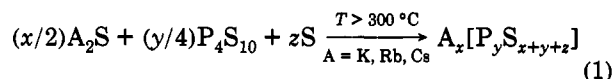
Received April 27, 1993

Revised Manuscript Received June 29, 1993

Recent advances in the development of alkali-metal polychalcogenide fluxes as reaction media at intermediate temperatures (200 < T < 500 °C) produced a variety of new ternary and quaternary chalcogenides.¹ This method is particularly useful in stabilizing structural fragments which are not stable at higher temperatures such as long S_x²⁻ (x = 4, 5, 6) units.² During our studies with polychalcogenides, we noticed that another set of main group structural units, namely the various thiophosphates [P_xS_y]ⁿ⁻ were also rather uncommon in their occurrence in solid-state compounds. With the exception of the important MPS₃ class of compounds,³ which contains the ethane-like [P₂S₆]⁴⁻ ligand, [P_xS_y]ⁿ⁻ containing solids are relatively few.⁴⁻⁶ Group 5 transition-metal thiophosphates have been reported and reviewed by Evain et al.⁷ These compounds exhibit structural diversity due to a variety of anionic P/S ligands and tendency for low dimensionality. Transition-metal thiophosphates are of potential importance as low-dimensional cathode materials for secondary lithium batteries.⁸ Metal thiophosphates are typically

synthesized by direct combination of the elements at high temperature (500–800 °C). It has been noted that complicated Lewis acid–base equilibria exist among [P₂S₆]⁴⁻, [P₂S₅]²⁻, [P₂S₇]⁴⁻, and [PS₄]³⁻ ligands at high temperatures.⁹ To date, very little effort has been invested in the synthesis of quaternary metal thiophosphate compounds at intermediate temperatures. Thus, we are interested to develop a general methodology by which new thiophosphate (or chalcophosphate) compounds can be consistently obtained in a similar fashion that we have observed in polychalcogenides. Here we report the use of novel low-melting (300–400 °C) alkali-metal polythiophosphate fluxes to synthesize new quaternary metal thiophosphates. This temperature window should allow access to new, metastable compounds that may not be thermodynamically stable at higher temperatures. The recently reported RbVP₂S₇ was prepared at 550 °C and is a notable example.¹⁰ We have applied this new molten salt flux to group 15 (Bi and Sb) metals and application to other p-block elements and transition metals seems very promising.¹¹ Using these fluxes, we prepared the new compounds KBiP₂S₇ and RbBiP₂S₇ which feature a new layered structure type containing the pyrothiophosphate building block. Their structural characterization and optical properties are reported.

The formation of molten alkali-metal thiophosphate fluxes results from the fusion of alkali-metal sulfide, phosphorous pentasulfide, and elemental sulfur (see eq 1).



We view the A_x[PS_y] fluxes as a significant variation over the A₂S_x fluxes in that they provide not just P atoms but excess [P_xS_y]ⁿ⁻ anions which act as mineralizers. In other words, the acid/base characteristics of the A_x[PS_y] fluxes are very different from those of the A₂S_x fluxes in that they tend to be more basic.¹ The chemical properties of these melts can be controlled by the ratios of their constituent elements. The relatively good solubility properties of A_n[P_xS_y] salts in water and organic solvents allow for easy isolation of products.

KBiP₂S₇ was synthesized from a mixture of Bi/P₄S₁₀/K₂S/S (1:1.5:2:4) at 400 °C.¹² The structure¹³ of ABiP₂S₇ is layered and shown in Figure 1a. It represents a complex new structure type. The corrugated layers are separated by eight-coordinate K⁺ ions (K–S mean = 3.34(6) Å). Another view of KBiP₂S₇ is shown in Figure 1b. The layers are assembled from Bi³⁺ and [P₂S₇]⁴⁻ units forming irregular eight-membered Bi–S–P rings. The P(2)–S₄ tetrahedron of the pyrothiophosphate ligand [P₂S₇]⁴⁻ coordinates in a bidentate fashion to Bi and acts as a bridge to a second Bi to form the top side of the eight-membered ring. The Bi atoms are connected at the bottom of the ring by the P(2)–S₄ tetrahedron of a second P₂S₇ group that acts as a tridentate to both Bi atoms. The bridging mode of the [P₂S₇]⁴⁻ fragment is rather complicated and

[†] A. P. Sloan Foundation Fellow 1991–93 and Camille and Henry Dreyfus Teacher Scholar 1993–95.

(1) (a) Kanatzidis, M. G. *Chem. Mater.* 1990, 2, 353–363. (b) Kanatzidis, M. G.; Park, Y. *Chem. Mater.* 1990, 2, 99–101. (c) Zhang, X.; Kanatzidis, M. G., manuscript in preparation.

(2) (a) Kanatzidis, M. G.; Park, Y. *J. Am. Chem. Soc.* 1989, 111, 3767–3769. (b) Park, Y.; Kanatzidis, M. G. *Angew. Chem., Int. Ed. Engl.* 1990, 29, 914–915. (c) Liao, J. H.; Varotsis, C.; Kanatzidis, M. G. *Inorg. Chem.* 1993, 32, 2453–2462.

(3) (a) Hahn, H.; Klingens, W. *Naturwissenschaften* 1965, 52, 494. (b) Hahn, H.; Ott, R.; Klingens, W. *Z. Anorg. Allg. Chem.* 1973, 396, 271–278.

(4) An earlier claim of the existence of the M₃(PS₄)₂ (M = first-row transition metals) general class of compounds proved incorrect. The reported XRD powder patterns for these materials are identical to those of MPS₃. (a) Diehl, R.; Carpentier, C.-D. *Acta Crystallogr.* 1973, B29, 1097–1105. (b) Buck, P.; Carpentier, C.-D. *Acta Crystallogr.* 1973, B29, 1864–1868. (c) Zimmerman, H.; Carpentier, C.-D.; Nitsche, R. *Acta Crystallogr.* 1975, B31, 2003–2006. (d) Becker, R.; Brockner, W.; Eisenmann, B. *Z. Naturforsch.* 1987, 42a, 1309–1312. (e) Ferrari, A.; Cavalca, L. *Gazz. Chim. Ital.* 1948, 78, 283–285. (f) Diehl, R.; Carpentier, C.-D. *Acta Crystallogr.* 1977, B33, 1399–1404. (g) Simon, A.; Peters, K.; Peters, E.-M.; Hahn, H. *Z. Naturforsch.* 1983, 38b, 426–427. (h) Jansen, M.; Henseler, U. *J. Solid State Chem.* 1992, 99, 110–119.

(5) (a) Toffoli, P.; Rouland, J. C.; Khodadad, P.; Rodier, N. *Acta Crystallogr.* 1985, C41, 645–647. (b) Toffoli, P.; Khodadad, P.; Rodier, N. *Acta Crystallogr.* 1982, B38, 2374–2378. (c) Toffoli, P.; Khodadad, P.; Rodier, N. *Bull. Soc. Chim. Fr.* 1981, 11, 429–432.

(6) (a) Mercier, R.; Malugani, J.-P.; Fahys, B.; Robert, G. *Acta Crystallogr.* 1982, B38, 1887–1890. (b) Fiechter, S.; Kuhs, W. F.; Nitsche, R. *Acta Crystallogr.* 1980, B36, 2217–2220. (c) Schafer, H.; Schafer, G.; Weiss, A. *Z. Naturforsch.* 1965, 20b, 811. (d) Brec, R.; Evain, M.; Grenouilleau, P.; Rouxel, J. *Rev. Chim. Min.* 1983, 20, 283–294. (e) Brec, R.; Grenouilleau, P.; Evain, M.; Rouxel, J. *Rev. Chim. Min.* 1983, 20, 295–304. (f) Evain, M.; Lee, S.; Queignec, M.; Brec, R. *J. Solid State Chem.* 1987, 71, 139–153. (g) Jandali, M. Z.; Eulenberger, G.; Hahn, H. *Z. Anorg. Allg. Chem.* 1985, 530, 144–154. (h) Weiss, A.; Schafer, H. *Z. Naturforsch.* 1963, 18b, 81–82.

(7) Evain, M.; Brec, R.; Whangbo, M.-H. *J. Solid State Chem.* 1987, 71, 244–262.

(8) Thompson, A. H.; Whittingham, M. S. U.S. Patent 4,049,879, 1977.

(9) Menzel, F.; Ohse, L.; Brockner, W. *Heteroatom Chem.* 1990, 1(5), 357–362.

(10) Durand, E.; Evain, M.; Brec, R. *J. Solid State Chem.* 1992, 102, 146–155.

(11) McCarthy, T. J.; Kanatzidis, M. G., submitted for publication.

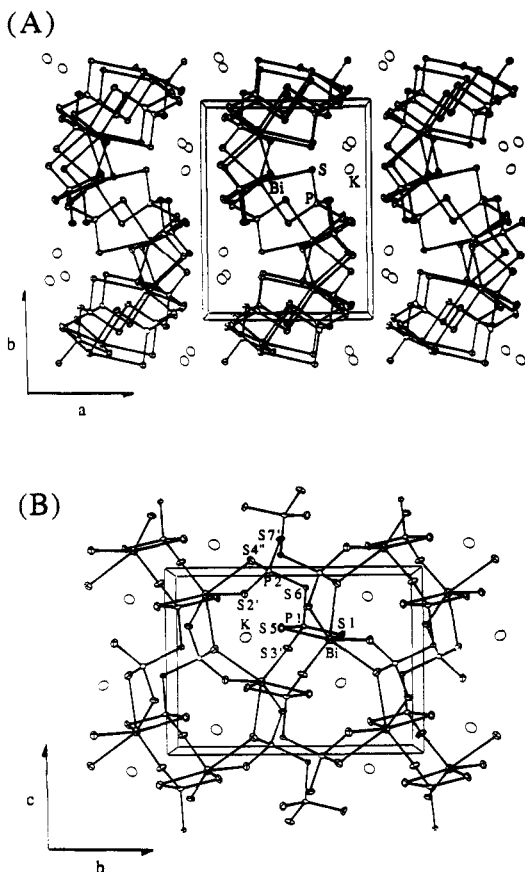
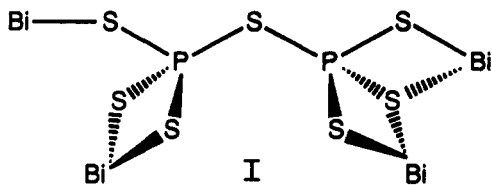


Figure 1. (A) ORTEP packing diagram of KBiP₂S₇ looking down the *c* axis with labeling. (B) ORTEP representation and labeling of the KBiP₂S₇ layer looking down the *a* axis. Selected distances are as follows: P(1)–S(1) 2.003(3), P(1)–S(3)' 2.035(3), P(1)–S(5) 2.018(3), P(1)–S(6) 2.115(3), P(2)–S(2)' 2.015(3), P(2)–S(4)'' 2.016(3), P(2)–S(6) 2.111(3), P(2)–S(7)' 2.024(3) Å. Selected angles are as follows: P(1)–S(6)–P(2) 111.2(1), S(1)'–P(1)–S(6) 100.4(1), S(3)'–P(1)–S(5) 109.6(1), S(7)'–P(2)–S(6) 98.2(1), S(2)'–P(2)–S(4)'' 108.1(1).

it is illustrated in I. The rings are connected in two dimensions by P–S–Bi linkages to form the layer. The



(12) KBiP₂S₇ was synthesized from a mixture of 0.031 g (0.15 mmol) of Bi, 0.050 g (0.225 mmol) of P₄S₁₀, 0.033 g (0.30 mmol) of K₂S, and 0.019 g (0.60 mmol) of S. This mixture was sealed under vacuum in a Pyrex tube and heated to 400 °C for 4 days followed by cooling to 110 °C at 4 °C/h. The excess yellow-colored K₂P₂S₇ matrix was removed from the red crystals (68% yield) with dimethylformamide (DMF). The crystals are air and water stable. Single crystals of the isostructural Rb analogue were also synthesized under the same conditions, except at 420 °C (57% yield). The compound was found to be isostructural to KBiP₂S₇ by powder X-ray diffraction. Quantitative microprobe analysis on red crystals gave Rb_{1.0}Bi_{1.2}P_{1.9}S_{7.4} (average of three data acquisitions).

(13) Crystal data for KBiP₂S₇ at 20 °C (Mo K α radiation): *a* = 9.500(3) Å, *b* = 12.303(4) Å, *c* = 9.097(3) Å, β = 90.59(3)°, *V* = 1063.1(6) Å³, *Z* = 4, *D*_{calc} = 3.339 g/cm³, space group P2₁/c (no. 14), *2* θ _{max} = 50°, total data collected, 2192; unique data (averaged), 2060; data with *F*_o² > 3 σ (*F*_o²), 1672. The structure was solved using SHELXS-86 (direct methods).¹⁴ An empirical absorption correction based on ψ scans was applied to the data, followed by a (DIFABS)¹⁵ correction to the isotropically refined data. Complete anisotropic refinement (100 variables) resulted in a final *R*/*R*_w = 2.8/3.1%.

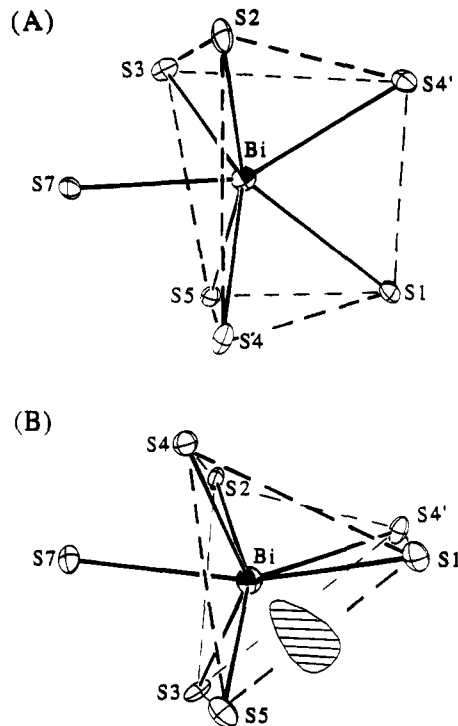


Figure 2. (A) ORTEP representation and labeling of the Bi–S coordination site. The polyhedron is outlined with dotted lines for clarity. Selected distances are as follows: Bi–S(1) 3.047(2), Bi–S(2) 2.867(2), Bi–S(3) 2.761(2), Bi–S(4) 2.930(2), Bi–S(4)' 2.971(2), Bi–S(5) 2.906(2), Bi–S(7) 2.820(2). Selected angles are as follows: S(1)–Bi–S(2) 125.46(5), S(1)–Bi–S(3) 138.29(5), S(4)'–Bi–S(5) 130.43(6), S(4)–Bi–S(4)' 113.69(5), S(1)–Bi–S(4) 71.58(6), S(1)–Bi–S(4)' 70.16(5), S(3)–Bi–S(7) 74.76(6), S(4)–Bi–S(7) 70.04(6), S(3)–Bi–S(5) 93.25(6), S(4)–Bi–S(5) 78.63(5). (B) ORTEP representation and labeling of the BiS₇ polyhedron viewed from the top of the capped trigonal prism. The probable location of the Bi³⁺ lone pair is shown.

layers stack with their eight-membered rings in registry so that they form channels running down the *a* axis.

Bi is coordinated by seven S atoms to form a distorted capped trigonal prism (see Figure 2a). The distances range from 2.761(2) to 3.047(2) Å which compare well with those found in BiPS₄.^{4c} The coordination geometry is distorted because of the stereochemically active 6s² lone pair of Bi³⁺. The S(7) atom caps one of the three rectangular faces of the trigonal prism. The lone pair presumably caps one of the other two faces. Inspection of the angles of the face, defined by S(2), S(4), S(1), S(4)' (see Figure 2b), reveal S(1)–Bi–S(2) and S(4)–Bi–S(4)' angles of 125.46(5)° and 113.69(5)°, respectively. The S(1)–Bi–S(3) and S(4)'–Bi–S(5) angles of the second face, defined by S(3), S(4)', S(5), S(1), are larger at 138.29(5)° and 130.43(6)°, respectively, and are probably due to the repulsive effect of the lone pair and the atoms. Each capped trigonal prism shares three edges and one corner with the terminal sulfides of four [P₂S₇]⁴⁻ ligands.

ABiP₂S₇ is structurally quite different from RbVP₂S₇, which also possesses a layered structure. The major differences are in the coordination number and geometry of the M³⁺ atom, and bonding modes of the [P₂S₇]⁴⁻ fragment. Furthermore, the sheets of ABiP₂S₇ are cor-

(14) Sheldrick, G. M. In *Crystallographic Computing 3*; Sheldrick G. M., Kruger, C., Daddard, R., Eds.; Oxford University Press: Oxford, England, 1985; pp 175–189.

(15) Walker, N.; Stuart, D. *Acta Crystallogr.* 1983, A39, 158–166.

rugated. The stereochemically active lone pair of Bi^{3+} also influences the structure of the layers by distorting the BiS_7 polyhedron. The potential multiple denticity of the $[\text{P}_2\text{S}_7]^{4-}$ ligand suggests that a large number of new solid-state structures may be possible with various main-group and transition metals. The $[\text{P}_2\text{S}_7]^{4-}$ ligand has been observed in $\text{Ag}_7(\text{PS}_4)(\text{P}_2\text{S}_7)$,^{5b} RbVP_2S_7 ,¹¹ $\text{Ag}_4\text{P}_2\text{S}_7$,¹⁶ $\text{Hg}_2\text{P}_2\text{S}_7$,¹⁷ and $\text{As}_2\text{P}_2\text{S}_7$.¹⁸

The optical properties of KBiP_2S_7 and RbBiP_2S_7 suggest that they are medium bandgap semiconductors.¹⁹ The optical absorption spectrum of KBiP_2S_7 is shown in Figure 3 and exhibits a steep absorption edge from which the bandgap, E_g , can be estimated at 2.25 eV. Two absorptions at 2.67 and 3.47 eV are readily resolved and are tentatively assigned to electronic $\text{S} \rightarrow \text{Bi}$ charge-transfer transitions. The bandgap of RbBiP_2S_7 is also 2.25 eV. The far-IR spectrum of the compound shows the characteristic absorbances of the $[\text{P}_2\text{S}_7]^{4-}$ ligand.²⁰

In conclusion, the synthesis of new quaternary thiophosphate compounds with alkali metal polythiophosphate molten salts is an interesting and promising synthetic

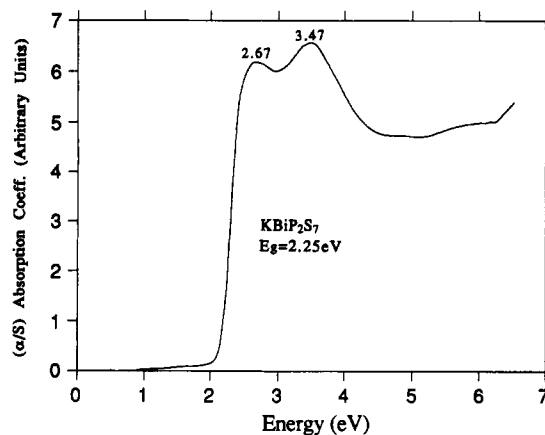


Figure 3. Optical absorption spectrum of KBiP_2S_7 .

method that is potentially broadly applicable to most metal systems. A number of other new A/M/P/Q (A = K, Rb, Cs; M = Bi, Sb; Q = S, Se) compounds have been synthesized with this method and have been structurally characterized.²⁴ The relatively low melting temperatures of the $\text{A}_x[\text{PS}_y]$ fluxes not only should favor metastable structures but more importantly provide a reliable method for stabilization of $[\text{P}_x\text{S}_y]^{n-}$ units. The various flux characteristics favoring formation of a particular $[\text{P}_x\text{S}_y]^{n-}$ anion are under investigation.

Acknowledgment. We wish to gratefully acknowledge the financial support of NSF (DMR-9202428).

Supplementary Material Available: Listings of powder diffraction patterns, positional parameters, B and U values, and intermolecular bond distances and angles for KBiP_2S_7 (20 pages); list of observed and calculated structure factors for KBiP_2S_7 (12 pages). Ordering information is given on any current masthead page.

(16) Toffoli, P.; Khodadad, P.; Rodier, N. *Acta Crystallogr.* 1977, B33, 1492-1494.

(17) Jandali, M. Z.; Eulenberger, G.; Hahn, H. Z. *Anorg. Allg. Chem.* 1978, 445, 184-192.

(18) Honle, W.; Wibbelmann, C.; Brockner, W. Z. *Naturforsch.* 1984, 39b, 1088-1091.

(19) (a) Absorption data were calculated from the reflectance data using the Kubelka-Munk function $\alpha/S = (1 - R)^2/2R$, where R is the reflectance at a given wavelength, α is the absorption coefficient, and S is the scattering coefficient. The scattering coefficient has been shown to be practically wavelength independent for particles larger than $5 \mu\text{m}$ which is smaller than the particle size of the samples used here. BaSO_4 powder was used as reference (100% reflectance). (b) Wendlandt, W. W.; Hecht, H. G. *Reflectance Spectroscopy*; Interscience Publishers: New York, 1966. (c) Kotum, G. *Reflectance Spectroscopy*; Springer Verlag: New York, 1969. (d) Tandon, S. P.; Gupta, J. P. *Phys. Status Solidi* 1970, 38, 363-367.

(20) The solid state far-IR spectrum of KBiP_2S_7 in a CsI matrix shows absorbances at 600 (s), 583 (s), 576 (ssh), 564 (msh), 557 (msh), 526 (wsh), 464 (vs), 412 (w) cm^{-1} .²¹ The very strong absorbance at 464 cm^{-1} represents the characteristic P-S-P stretching vibration while the remaining absorbances are due to $-\text{PS}_3$ stretching vibrations by analogy to $\text{Ag}_4\text{P}_2\text{S}_7$.^{9,22} A second set of absorbances at 300 (vw), 270 (wsh), 250 (msh), 247 (m), 238 (msh), 227 (wsh), 208 (wsh), 203 (wsh), 192 (vw), 174 (vw), 169 (vw), 157 (vw), and 149 (vw) cm^{-1} are assigned to Bi-S stretching vibrations and P-S deformation modes.^{9,22,23}

(21) Abbreviations: s = strong, m = medium, w = weak, sh = shoulder, v = very.

(22) (a) Queignec, M.; Evain, M.; Brec, R.; Sourisseau, C. *J. Solid State Chem.* 1986, 63, 89-109. (b) Andrae, H.; Blachnik, R. *J. Alloys Compounds* 1992, 189, 209-215.

(23) D'ordyai, V. S.; Galagovets, I. V.; Peresh, E. Yu.; Voroshilov, Yu. V.; Gerasimenko, V. S.; Slivka, V. Yu. *Russ. J. Inorg. Chem.* 1979, 24(11), 1603-1606.

(24) McCarthy, T. J.; Kanatzidis, M. G., manuscript in preparation.